ADVANCED FUNCTIONAL MATERIALS

# Supporting Information

for *Adv. Funct. Mater.*, DOI: 10.1002/adfm.202005200

# Flexible Color-Tunable Electroluminescent Devices by Designing Dielectric-Distinguishing Double-Stacked Emissive Layers

*Yong Zuo, Xiang Shi, Xufeng Zhou, Xiaojie Xu, Jun Wang, Peining Chen, Xuemei Sun,* and Huisheng Peng**

# Supporting Information

## Flexible color-tunable electroluminescent devices by designing dielectric-distinguishing double-stacked emissive layers

*Yong Zuo, Xiang Shi, Xufeng Zhou, Xiaojie Xu, Jun Wang, Peining Chen, Xuemei Sun*, Huisheng Peng**

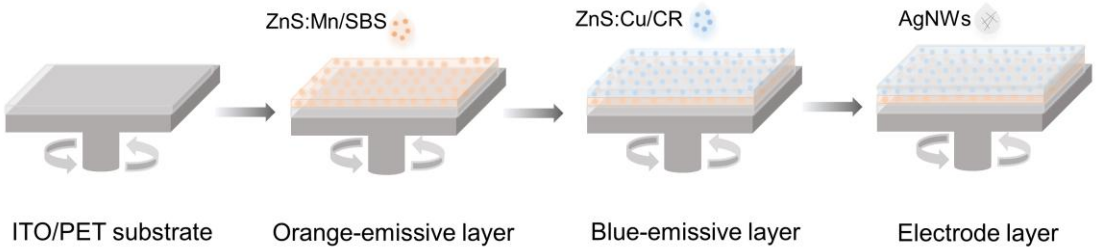


**Figure S1.** Schematic illustration of the sequential spin-coating process to fabricate the flexible color-tunable ACEL device.

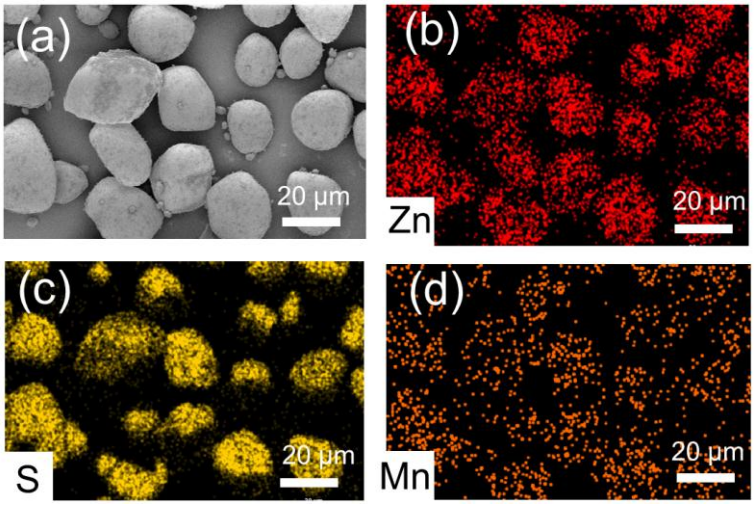


**Figure S2.** (a) SEM image of ZnS:Mn phosphors. (b-d) Dispersion of Zn, S and Mn elements, respectively.

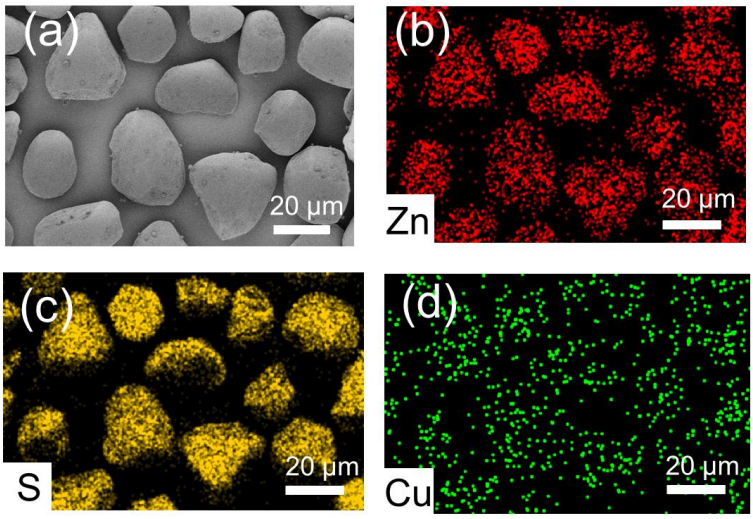


**Figure S3.** (a) SEM image of ZnS:Cu phosphors. (b-d) Dispersion of Zn, S and Cu elements, respectively.

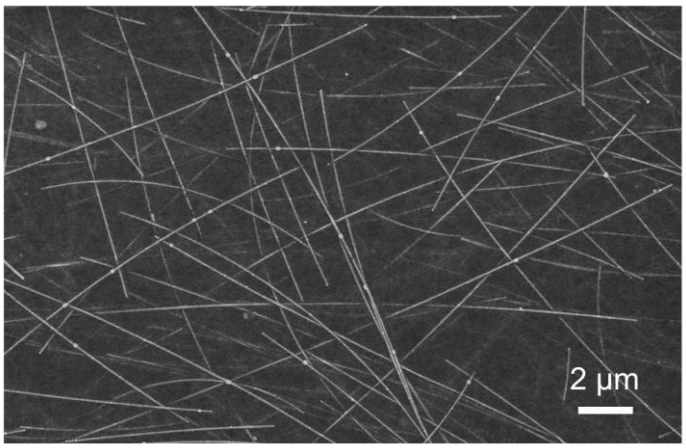


**Figure S4.** SEM image of the AgNWs top electrode.

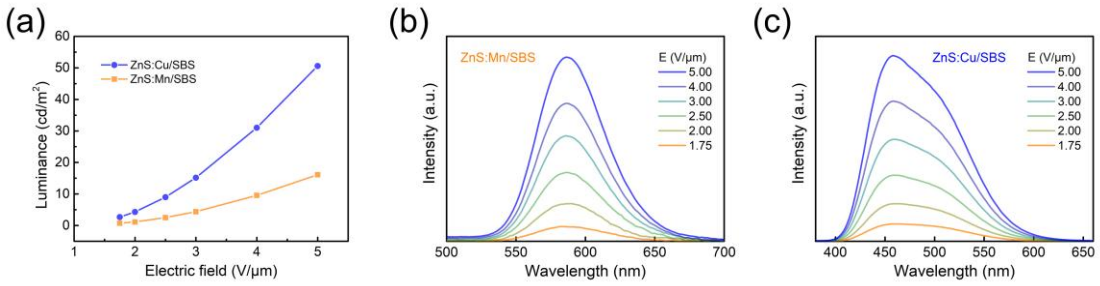


**Figure S5.** (a) Luminance and (b, c) EL spectra of the monochromatic devices with ZnS:Mn/SBS or ZnS:Cu/SBS emissive layer operated at varied electric fields.

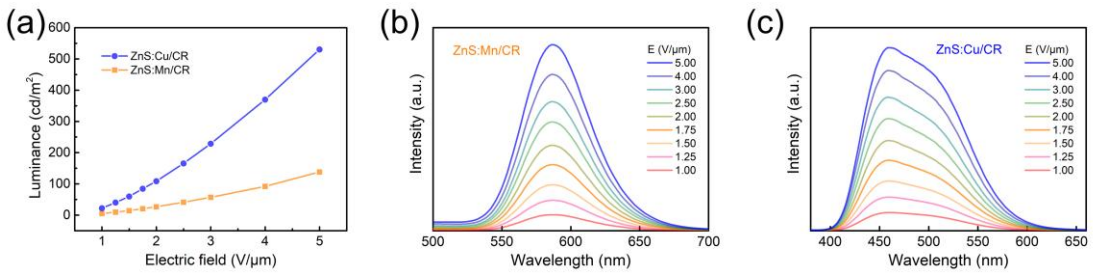


**Figure S6.** (a) Luminance and (b, c) EL spectra of the monochromatic devices with ZnS:Mn/CR or ZnS:Cu/CR emissive layer operated at varied electric fields.

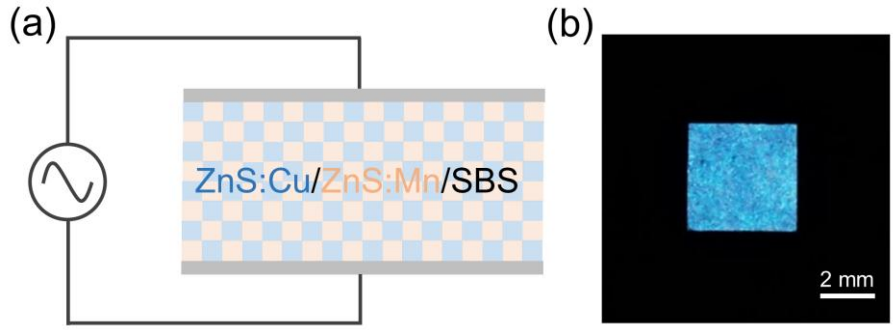


**Figure S7.** (a) Schematic structure and (b) photograph of the ACEL device with a single emissive layer (ZnS:Mn/ZnS:Cu/SBS) under an alternating electric field.

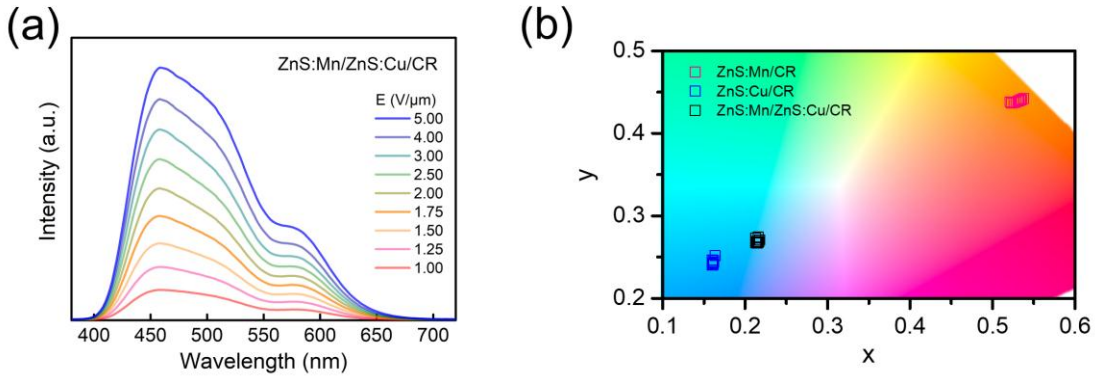


**Figure S8.** (a) EL spectra and (b) corresponding CIE coordinates of the ACEL device with a single emissive layer (ZnS:Mn/ZnS:Cu/CR) operated at varied electric fields.

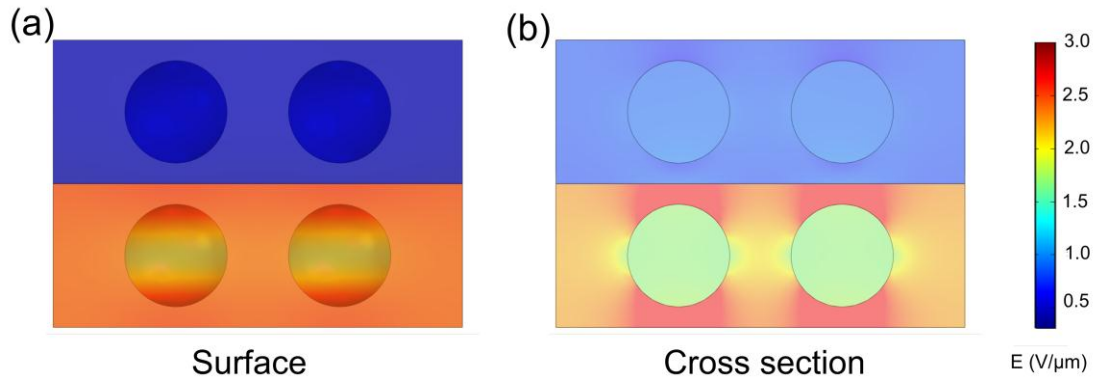


**Figure S9.** Simulation of electric field distribution on the (a) surface and (b) cross section of the ACEL device with double-stacked emissive layers.

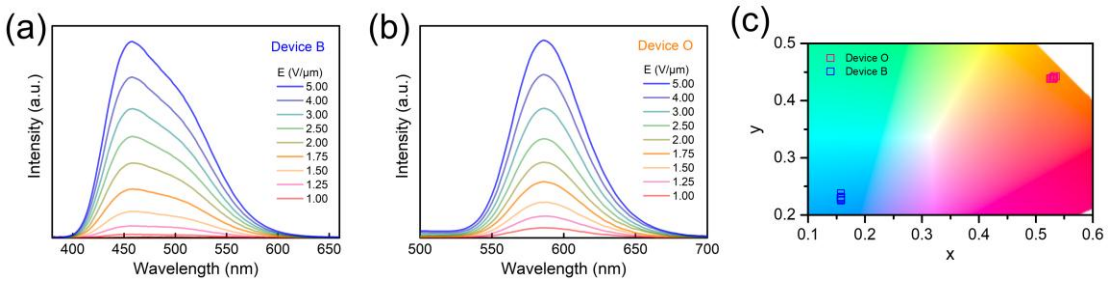


**Figure S10.** EL spectra of (a) Device B and (b) Device O operated at varied electric fields. (c) Corresponding CIE coordinates of Device B and O at varied electric fields.

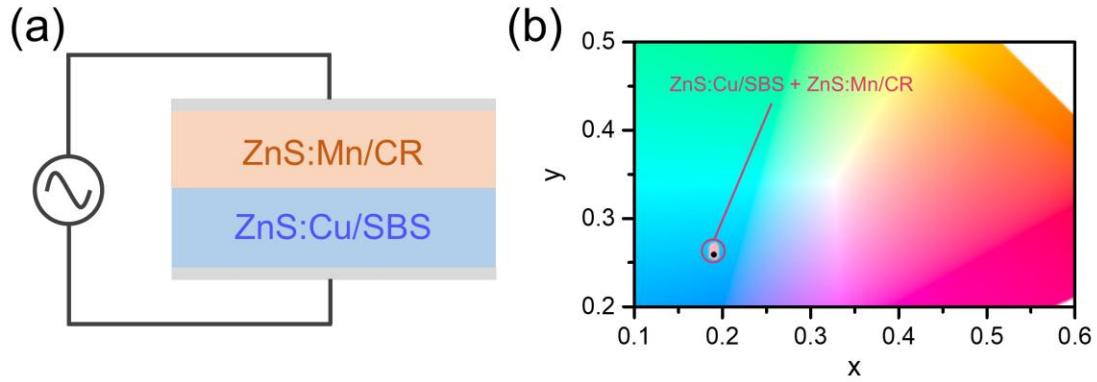


**Figure S11.** (a) Schematic structure of the ACEL device with blue-emissive layer of ZnS:Cu/SBS composites and orange-emissive layer of ZnS:Mn/CR composites. (b) CIE coordinates of the device operated at varied electric fields.

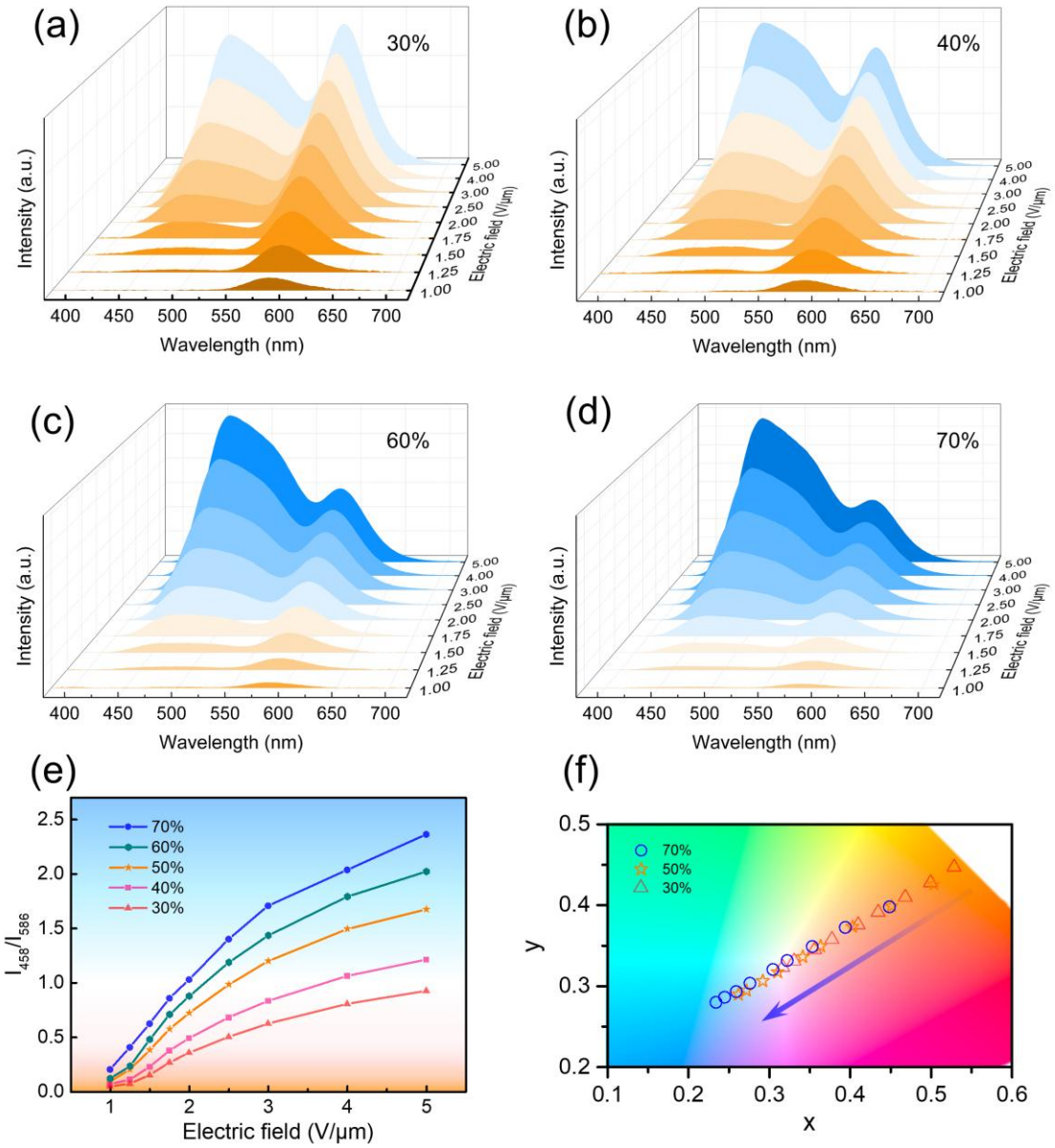


**Figure S12. Color-tuning performance of the ACEL device with different contents of ZnS:Cu phosphors.** (a-d) EL spectra of the ACEL with ZnS:Cu phosphors contents of (a) 30%, (b) 40%, (c) 60%, (d) 70% operated at varied electric fields and at the frequency of 2 kHz. (e) $I_{458}/I_{586}$ value and (f) corresponding CIE coordinates of the ACEL devices with different contents of ZnS:Cu phosphors at varied electric fields.

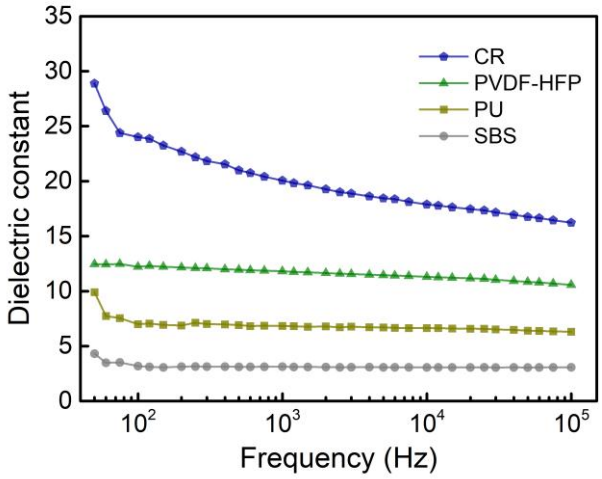


**Figure S13.** Frequency-dependent dielectric constant of CR, PVDF-HFP, PU and SBS.

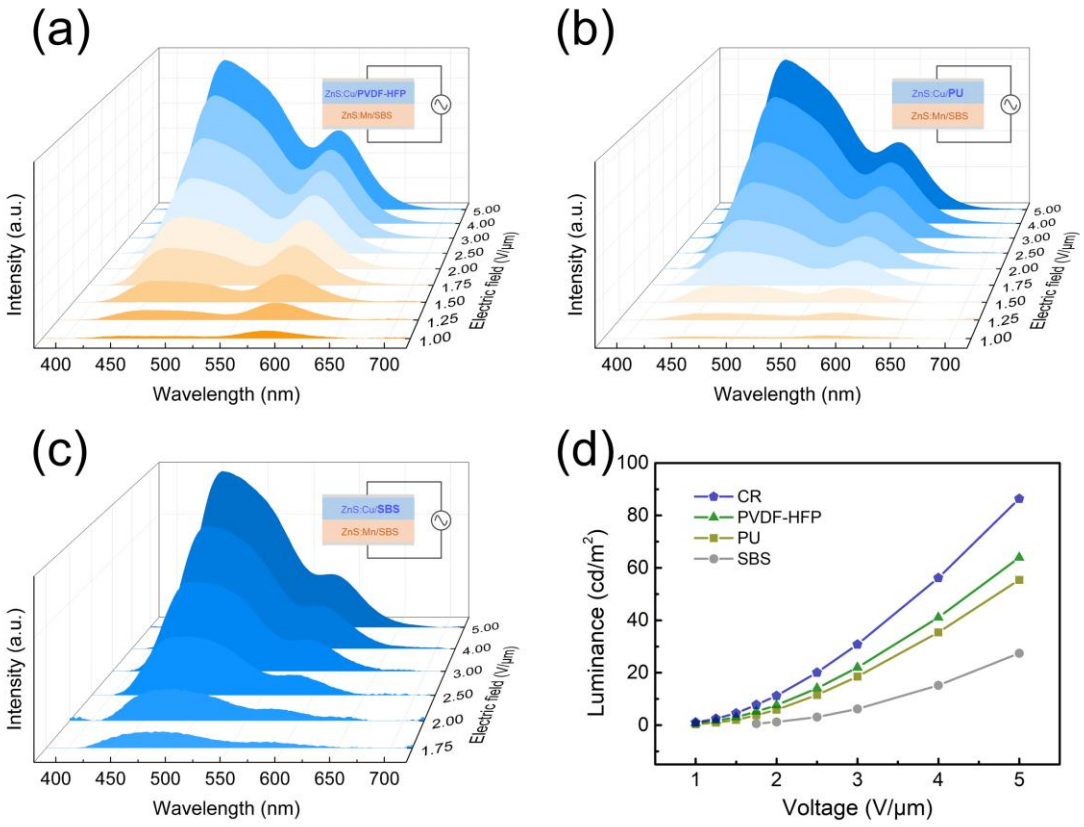


**Figure S14.** EL spectra of the ACEL devices using (a) PVDF-HFP, (b) PU and (c) SBS as polymer matrices in blue-emissive layer operated at varied electric fields and at the frequency of 2 kHz. (d) Luminance of the corresponding ACEL devices operated at varied electric fields.

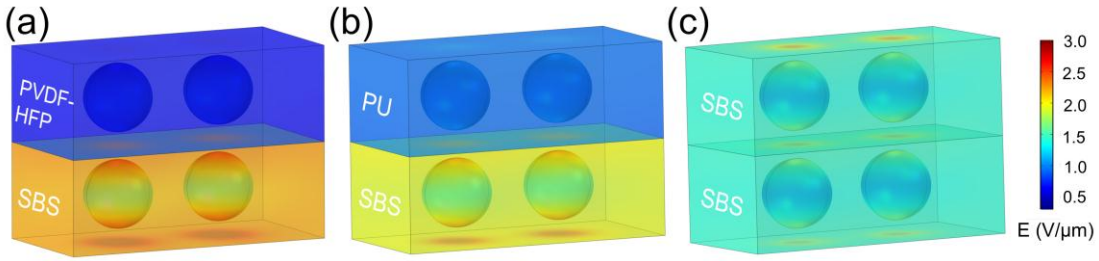


**Figure S15.** Simulation of electric field distribution in the ACEL devices using (a) PVDF-HFP, (b) PU and (c) SBS as polymer matrices in blue-emissive layer.

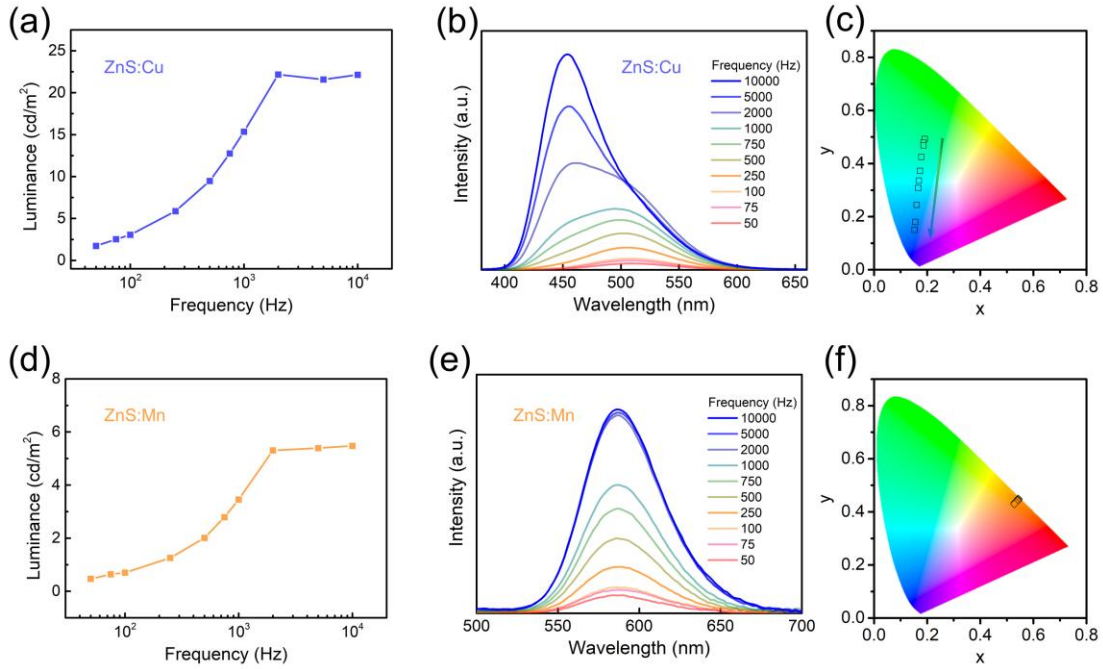


**Figure S16.** (a) Luminance, (b) EL spectra and (c) corresponding CIE coordinates of the monochromatic devices with ZnS:Cu/CR at varied frequencies. (d) Luminance, (e) EL spectra and (f) corresponding CIE coordinates of the monochromatic devices with ZnS:Mn/CR at varied frequencies.

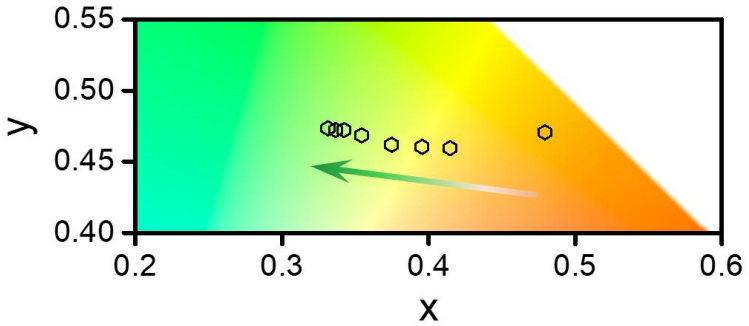


**Figure S17.** CIE coordinates of the ACEL device using CR as polymer matrix in blue-emissive layer operated at varied electric fields and at the frequency of 50 Hz.

**Table S1.** CIE coordinates of the ACEL devices with a single emissive layer at varied electric fields.

| E (V/μm) | ZnS:Mn/SBS CIE(x,y) | ZnS:Cu/SBS CIE(x,y) | ZnS:Mn/ZnS:Cu/SBS CIE(x,y) |
|---|---|---|---|
| 1.75 | （0.5400, 0.4462） | （0.1580, 0.2413） | （0.2298, 0.2852） |
| 2.00 | （0.5416, 0.4476） | （0.1591, 0.2392） | （0.2301, 0.2821） |
| 2.50 | （0.5392, 0.4423） | （0.1589, 0.2370） | （0.2328, 0.2815） |
| 3.00 | （0.5399, 0.4449） | （0.1587, 0.2356） | （0.2330, 0.2803） |
| 4.00 | （0.5372, 0.4423） | （0.1591, 0.2345） | （0.2315, 0.2780） |
| 5.00 | （0.5358, 0.4416） | （0.1594, 0.2345） | （0.2297, 0.2768） |

**Table S2.** CIE coordinates of the ACEL devices with different contents of ZnS:Cu phosphors at varied electric fields.

| E (V/μm) | 30% CIE(x,y) | 40% CIE(x,y) | 50% CIE(x,y) | 60% CIE(x,y) | 70% CIE(x,y) |
|---|---|---|---|---|---|
| 1.00 | ( 0.5290, 0.4466 ) | ( 0.5214, 0.4410 ) | ( 0.5035, 0.4254 ) | ( 0.4996, 0.4412 ) | ( 0.4485, 0.3980 ) |
| 1.25 | ( 0.4997, 0.4275 ) | ( 0.4816, 0.4204 ) | ( 0.4511, 0.3986 ) | ( 0.4363, 0.4007 ) | ( 0.3942, 0.3725 ) |
| 1.50 | ( 0.4686, 0.4093 ) | ( 0.4419, 0.4000 ) | ( 0.4029, 0.3733 ) | ( 0.3801, 0.3681 ) | ( 0.3532, 0.3490 ) |
| 1.75 | ( 0.4348, 0.3909 ) | ( 0.4017, 0.3770 ) | ( 0.3634, 0.3491 ) | ( 0.3391, 0.3436 ) | ( 0.3222, 0.3316 ) |
| 2.00 | ( 0.4102, 0.3756 ) | ( 0.3776, 0.3631 ) | ( 0.3412, 0.3359 ) | ( 0.3181, 0.3317 ) | ( 0.3044, 0.3206 ) |
| 2.50 | ( 0.3778, 0.3572 ) | ( 0.3451, 0.3454 ) | ( 0.3105, 0.3173 ) | ( 0.2901, 0.3147 ) | ( 0.2763, 0.3037 ) |
| 3.00 | ( 0.3565, 0.3447 ) | ( 0.3250, 0.3340 ) | ( 0.2920, 0.3061 ) | ( 0.2733, 0.3043 ) | ( 0.2592, 0.2934 ) |
| 4.00 | ( 0.3309, 0.3303 ) | ( 0.3013, 0.3206 ) | ( 0.2718, 0.2945 ) | ( 0.2547, 0.2933 ) | ( 0.2449, 0.2861 ) |
| 5.00 | ( 0.3169, 0.3229 ) | ( 0.2885, 0.3140 ) | ( 0.2618, 0.2894 ) | ( 0.2451, 0.2883 ) | ( 0.2343, 0.2801 ) |

**Table S3.** CIE coordinates of the ACEL devices with different polymer matrices in blue-emissive layers at varied electric fields.

| E (V/μm) | CR CIE(x,y) | PVDF-HFP CIE(x,y) | PU CIE(x,y) | SBS CIE(x,y) |
|---|---|---|---|---|
| 1.00 | （0.5035, 0.4254） | （0.4198, 0.3877） | （0.3700, 0.3629） | NA |
| 1.25 | （0.4511, 0.3986） | （0.3645, 0.3564） | （0.3205, 0.3395） | NA |
| 1.50 | （0.4029, 0.3733） | （0.3339, 0.3383） | （0.2906, 0.3186） | NA |
| 1.75 | （0.3634, 0.3491） | （0.3140, 0.3265） | （0.2752, 0.3073） | （0.2206, 0.2860） |
| 2.00 | （0.3412, 0.3359） | （0.3013, 0.3184） | （0.2679, 0.3012） | （0.2185, 0.2802） |
| 2.50 | （0.3105, 0.3173） | （0.2828, 0.3073） | （0.2582, 0.2936） | （0.2187, 0.2770） |
| 3.00 | （0.2920, 0.3061） | （0.2706, 0.3004） | （0.2512, 0.2886） | （0.2198, 0.2751） |
| 4.00 | （0.2718, 0.2945） | （0.2568, 0.2930） | （0.2422, 0.2833） | （0.2197, 0.2734） |
| 5.00 | （0.2618, 0.2894） | （0.2496, 0.2906） | （0.2368, 0.2806） | （0.2178, 0.2717） |

**Table S4.** CIE coordinates of the color-tunable ACEL device at $E$ = 2 and 5 V/μm with different bending radii.

| Bending radius (mm) | E = 2 V/μm CIE(x,y) | E = 5 V/μm CIE(x,y) |
|---|---|---|
| ∞ | （0.3383, 0.3379） | （0.2624, 0.2927） |
| 13.5 | （0.3328, 0.3341） | （0.2571, 0.2872） |
| 7.5 | （0.3356, 0.3370） | （0.2622, 0.2920） |
| 5.0 | （0.3360, 0.3365） | （0.2581, 0.2880） |
| 3.8 | （0.3341, 0.3351） | （0.2574, 0.2875） |
| 3.0 | （0.3318, 0.3337） | （0.2555, 0.2862） |
| 2.5 | （0.3275, 0.3317） | （0.2553, 0.2864） |
| 2.0 | （0.3343, 0.3358） | （0.2579, 0.2879） |

**Table S5.** CIE coordinates of the color-tunable ACEL device at $E$ = 2 and 5 V/μm with different bending cycles.

| Bending cycle | E = 2 V/μm CIE(x,y) | E = 5 V/μm CIE(x,y) |
|---|---|---|
| 0 | （0.3384, 0.3407） | （0.2627, 0.2950） |
| 200 | （0.3358, 0.3370） | （0.2638, 0.2968） |
| 400 | （0.3330, 0.3366） | （0.2584, 0.2929） |
| 600 | （0.3333, 0.3356） | （0.2626, 0.2961） |
| 800 | （0.3330, 0.3337） | （0.2616, 0.2938） |
| 1000 | （0.3347, 0.3353） | （0.2627, 0.2942） |